J Electroceram (2006) 16:483–488
DOI 10.1007/s10832-006-9902-4

Structure and electrical properties of $Ba_{0.67}Sr_{0.33}TiO_3$ thin film fabricated by sol-gel based composite technique

Ling Ling Sun · Lay Im Tan · Ooi Kiang Tan · Zhi Hong Wang · Wei Guang Zhu

Abstract A sol-gel based novel technique is used to fabricate $Ba_{0.67}Sr_{0.33}TiO_3$ (BST) thin films with thickness up to several microns. In this technique, surface-modified fine BST particles are dispersed in a sol-gel precursor solution. The pH value of the precursor solution is modified to achieve high zeta potential for the dispersed powder, hence a very stable and uniform slurry can be produced. The slurry is then spin-coated onto Pt/Ti/SiO_2/Si substrate, pre-heated and annealed as in conventional sol-gel process. The resulting films show well-developed dense polycrystalline structure with uniform grain distribution. The metal-BST-metal structure of the films displays good dielectric properties.

Keywords BST · Sol-gel · Thin film

1 Introduction

In recent years $Ba_xSr_{1-x}TiO_3$ (BST) thin films have received intensive research interest for their device applications, such as bolometers [1–3], gas sensor [4, 5], tunable microwave filters [6] and radio-frequency microelectromechanical (RF-MEMS) capacitive switches [7]. For most of the cases, higher dielectric constant of BST makes it possible to achieve smaller size or better performance of the devices. In addition, lower loss tangent of BST enables lower dielectric loss of the devices. BST film exhibits thickness dependent dielectric constants and loss tangents; specifically, thicker BST films have larger dielectric constants and lower loss tangents [8]. Efforts have been made to prepare thicker and crack free BST films [9, 10].

L. L. Sun · L. I. Tan · O. K. Tan (✉) · Z. H. Wang · W. G. Zhu
School of Electrical and Electronic Engineering, Nanyang Technological University, Singapore 639798

Several methods have been developed to prepare ferroelectric thin films, such as RF sputtering, metal organic chemical vapor deposition (MOCVD), electron beam evaporation, pulse laser deposition, hydrothermal electrochemical method, and sol-gel deposition. Among these methods, sol-gel process is widely used due to its good reproducibility, low cost and the compatibility with IC processes. However, the main limit of sol-gel process is the maximum film thickness that can be achieved. It is difficult to deposit films with thickness up to 1 μm because of cracks formation.

This paper presents a modified sol-gel method to prepare crack free BST film with thickness up to several microns by dispersing high energy ball milled nanoparticles into sol-gel precursor solution to form a slurry which can be spin coated on substrates of interest. The detailed process procedure, microstructure and electrical properties will be introduced in the following sections.

2 Experiment

2.1 BST sol-gel precursor solution preparation

The sol-gel BST precursor solution was prepared using a conventional route starting from raw metal organic materials of titanium (IV) butoxide, barium acetate, and strontium acetate. Figure 1 illustrates the preparation of the precursor BST solution with a Ba/Sr ratio of 67:33. Titanium (IV) butoxide was mixed with acetylacetone in a molar ratio of 1:4 to form chelate complex for stabilization consideration. Then, barium acetate and strontium acetate powders were weighted and dissolved in acetic acid at around 60°C. De-ionized water was added in a molar ratio of 1:4 (M_{Ti}:M_{DI}) to promote the dissolution process.

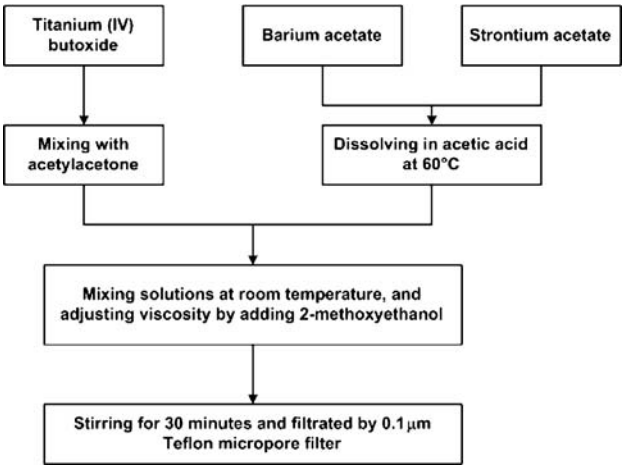

Fig. 1 Flow diagram for preparation of (Ba,Sr)TiO_3 sol-gel precursor solution

The dissolved (Ba,Sr) precursor solution was dripped into titanium butoxide precursor solution, and 2-methoxyethanol was added to achieve a final concentration of 0.2 M. The solution was filtered through a 0.1 μm Teflon micropore filter to remove dust and other suspended particles in solution.

2.2 High energy ball milling of BST powder

Commercial BST67/33 powder (from Kurt J. Lesker Company) was used as the particle source. High-energy ball milling technique was applied to reduce the particle size and promote the dispersion of particles in solution. A Fritsch "Pulverisette 5" planetary ball-milling machine (from Fritsch GmbH) was used. A container with tungsten carbide (93 wt% WC + 6 wt% Co, $\rho = 14.75$ g/cm) vials and balls were used. The vial has a volume of 250 ml with an inner diameter of 75 mm. The balls have diameters of 10 mm and 20 mm. The BST powder was used with a weight ratio of 1:20 to balls. The milling speed was set at 200 rpm. The milling was carried out in 30 minutes cycles with 20 min of milling followed by 10 min of pause to prevent the milling system from overheating. The milling was continued for 42 h. The powders were agglomerated after ball milling because of high surface energy of the powders. Hence a selected dispersant, organic vehicle (ESL #400), was added into the milled powders to modify the surface of the powder. The mass ratio of dispersant to powder was around 1:20. After the dispersant was added, the powder was ball milled for another 6 h to obtain a homogenous dispersion. Surface modified powder was collected after milling. FESEM observation and laser particle size analysis were carried out to estimate the particle size.

2.3 pH modification for BST sol-gel precursor solution and fabrication of slurry

The variation in pH of BST sol-gel precursor solution will result in a different zeta-potential being developed on the surface of the dispersed powder. This in turn can be used to alter the electrostatic forces between particles. When the absolute value of zeta potential is above 50 mV the dispersions are very stable due to mutual electrostatic repulsion; and when the zeta potential is close to zero, the coagulation (formation of larger assemblies of particles) is very fast and this causes a fast sedimentation.

The pH value of the BST precursor solution was varied between 2 and 11 by adding acetic acid the ammonium hydroxide. The pH modified BST sol-gel precursor solution was then added and mixed with the powder and was ball milled for another 12 h. The mass ratio of solution to powder was around 2:1. Zeta-potential measurement and sedimentation test were carried out to study the stability of the slurries with different pH values.

2.4 Film deposition and characterization

The films were obtained by the spin coating technique. Before the BST composite film deposition, a pure sol-gel layer was deposited as a buffer layer to enhance adhesion between composite film and substrate. A final capping layer of pure sol-gel film was applied to fill the micro-cracks on the composite film. Each layer was spun on at 2000 rpm for 30 s, then dried at 200°C and pyrolyzed at 400°C for 2 min. For all the films, 3 composite layers were deposited to achieve the film thickness around 3 microns. The final spin coated film was annealed for 1 h at 650°C in an oven in air.

The crystallization and microstructure of the films were studied using XRD and FESEM. The leakage current density of the films were measured using an HP4155B Semiconductor Parameter Analyzer. The measurements of the dielectric constant and dielectric loss were carried out using an HP4284A Precision LCR Meter.

3 Results and discussions

3.1 Powder characterization

3.1.1 Particle size observation

Figure 2 shows the FE-SEM images of BST powder, (a) raw powder and (b) high energy ball milled powder. Figure 3 shows the particle size distribution analyzed by a laser particle size analyzer. It is shown that the particle size of the raw powder is around 650 nm. After high energy ball milling for 48 h the particle size shows two distributions. Most of the

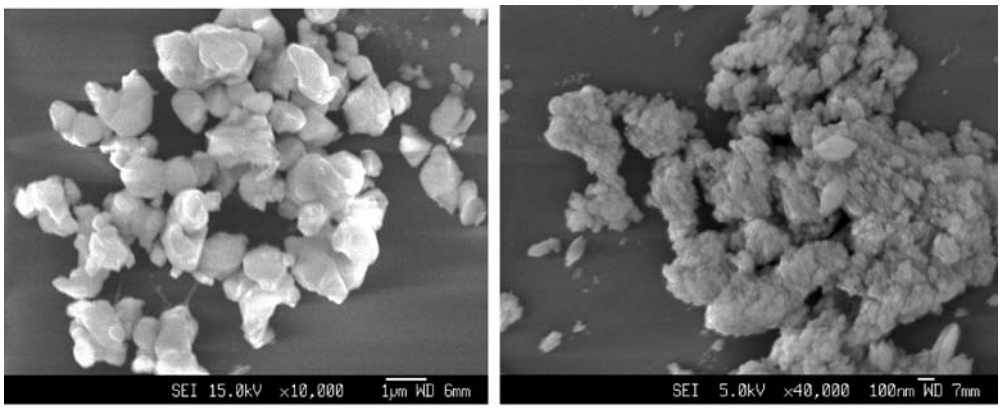

Fig. 2 FE-SEM images for BST powder (×10,000), (a) raw powder, (b) high energy ball milled powder

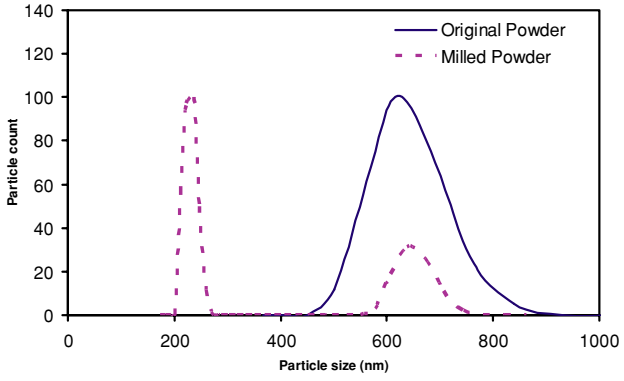

Fig. 3 Particle size distribution for original powder (solid line) and high energy ball milled powder (milled powder)

particles have reduced size of around 230 nm. Small amount of particles maintain original size. It is believed that the smaller particle size is beneficial to achieve denser and smoother film.

3.2 Stabilization conditions

3.2.1 Zeta potential

For 0.2 M BST sol-gel precursor solution, pH value varied from 1.2 to 6.5 depending on the volume ratio of acetic acid and MOE added. The pH was further adjusted up to 11 by adding ammonium hydroxide. In Fig. 4 the zeta potential of the BST particles as a function of pH is presented. An isoelectric point (IEP) is found at pH∼2.5. The highest absolute zeta potential value is presented in the basic pH region. Therefore, stabilization is probable at these pH values.

3.2.2 Sedimentation test

Sedimentation curves for pH of 2, 3.75 and 8.25 are shown in Fig. 5. Some time after pouring the slurry into the test tube,

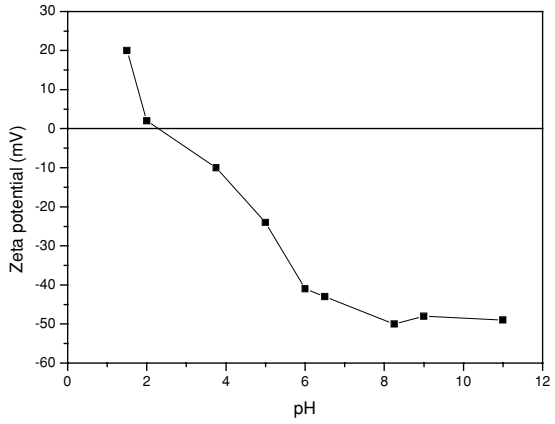

Fig. 4 Zeta potential against pH in aqueous suspension of high energy ball milled BST powder

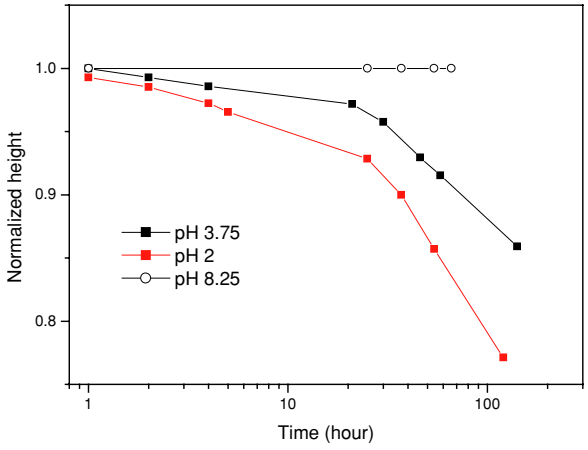

Fig. 5 Sedimentation test for BST powder suspended in BST sol-gel precursor solution

an interface was evident between a perfectly clear region, at the top of the tube, and a cloudy region at the bottom of the tube. The height of such interface was measured as a function of the elapsed time. The sedimentation test results are

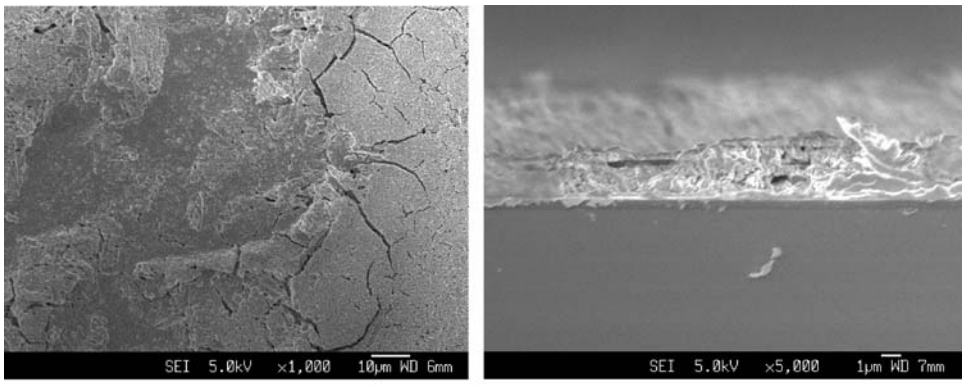

(a) Surface morphology (left) and cross section (right) with pH 2

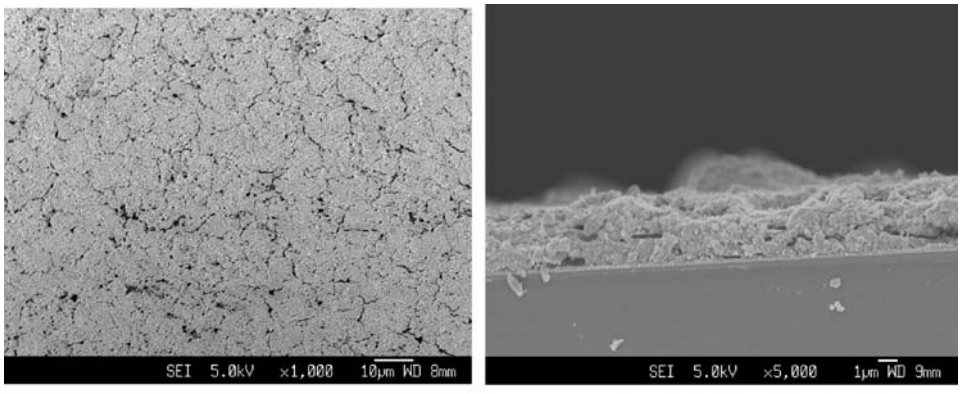

(b) Surface morphology (left) and cross section (right) with pH 3.75

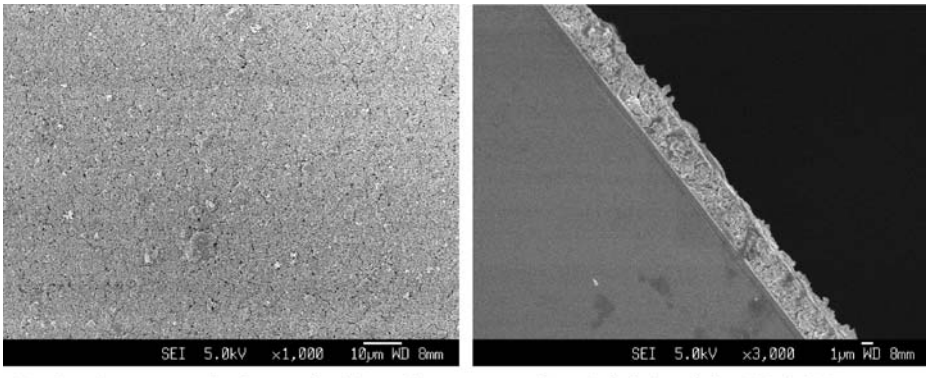

(c) Surface morphology (left) and cross section (right) with pH 8.25

Fig. 6 FESEM pictures of surface morphology and cross section of the films deposited using slurry with different pH value (a) pH 2, (b) pH 3.75 and (c) pH 8.25

consistent with zeta potential measurement results. For pH of 2, the zeta potential of the suspension is near IEP, therefore sedimentation happened very fast. For pH of 8.25, the slurry is very stable. No significant sedimentation happened even after 66 h of observation. The stability of the slurry with suspension zeta potential of 3.75 is between those of pH of 2 and 8.25.

3.3 Film structure analysis

Figure 6 depicts the surface morphology of the films deposited using slurry with different pH values. For the film deposited using slurry pH of 2, very uneven surface was observed. That is because powder sedimentation already happened before spin coating. This will cause the non-uniform powder distribution on the film surface. For pH of 3.75, the film was better than that deposited using slurry with pH of 2, but micro cracks were still observed on the surface. The micro cracks are believed to be due to powder agglomeration during spin coating. For the film deposited using the slurry with pH of 8.25, denser and smoother surface was obtained and no micro cracks were observed. Figure 6 shows the FESEM pictures of the cross section of the films.

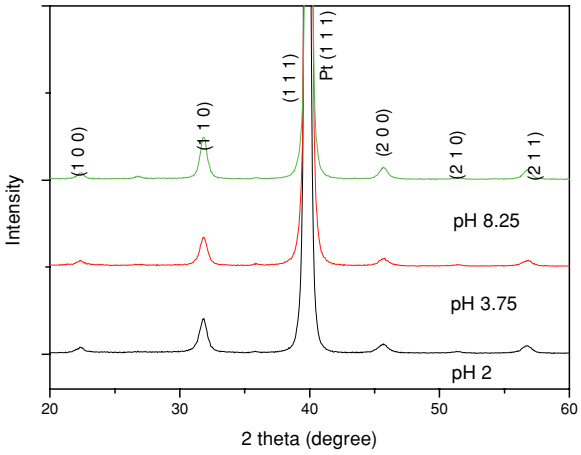

Fig. 7 XRD of films deposited using slurries with different pH values

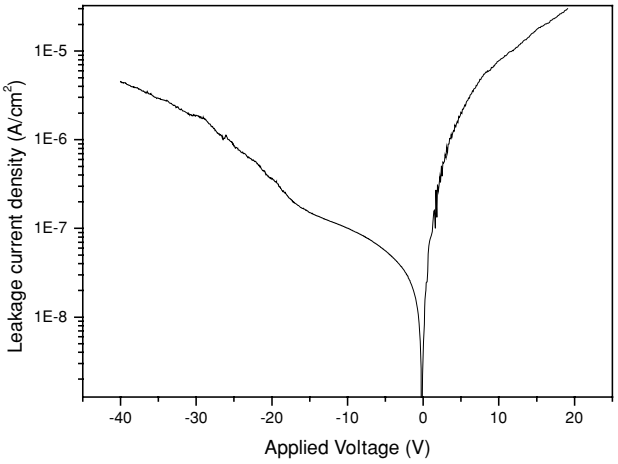

Fig. 8 I-V characteristic of BST composite film

Figure 7 shows the X-ray diffraction patterns of the films deposited using slurry with different pH values. All peaks can be identified for randomly oriented polycrystalline BST film.

3.4 Electric properties

3.4.1 Leakage current of BST composite film

The thickness of deposited BST thin film using pH 8.25 slurry is observed to be around 3 μm by SEM observation. E-beam evaporated Au layer was deposited as top electrode. The leakage current behaviors of the film were characterized at room temperature using an HP 4155B semiconductor parameter analyzer. Figure 8 illustrates the leakage current behavior. It is believed that the conduction behavior of Pt/sol-gel BST/Au thin film capacitors is generally dominated by the Schottky-barrier emission model, which has been commonly accepted in the publications [11]. For our sol-gel films, the leakage currents are asymmetric owing to the different top and bottom electrodes used. It is revealed that the composite film exhibits low leakage current and high dielectric breakdown voltage.

3.4.2 Dielectric properties of BST composite film

The dielectric properties of the BST composite film was investigated using an HP 4284A LCR meter at the frequency range from 10 Hz to 1 MHz. An oscillation level of 1 V was applied to Pt/BST/Au capacitors without bias.

It is shown in Fig. 9 the film exhibits the dielectric dispersion in the frequency range from 10 Hz to 1 MHz. It is believed the dielectric dispersion is due to the electronic defects in the film.

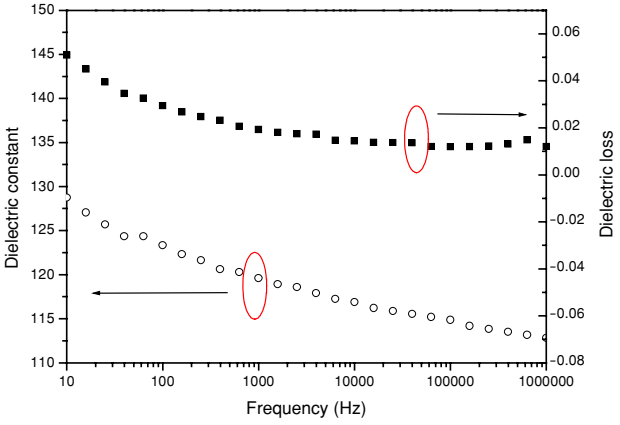

Fig. 9 Dielectric constant and dielectric loss versus the frequency for BST composite film

4 Summary

A sol-gel based composite technique is used to fabricate $Ba_{0.67}Sr_{0.33}TiO_3$ films with thickness up to several microns. In this technique, surface-modified fine BST particles were dispersed in a sol-gel precursor solution. The pH value of the precursor solution was modified to make the dispersed powder have high zeta potential, hence very stable and uniform slurry was produced. It is found that the film deposited using slurry with pH value of 8.25 has dense, crack free and well developed polycrystalline structure. The film exhibits low leakage current and high dielectric breakdown voltage. At 1 kHz, the dielectric constant and dielectric loss were measured to be 120 and 0.019.

References

1. K. Hashimoto, H. Xu, T. Mukaigawa, R. Kubo, H. Zhu, M. Noda, and M. Okuyama, *Sens. Actuat.* A **88**, 10 (2001).

2. M. Noda, K. Hashimoto, R. Kubo, H. Tanaka, T. Mukaigawa, H.P. Xu, and M. Okuyama, *Sens. Actuat.* A **77**, 39 (1999).
3. M. Noda, H. Xu, T. Mukaigawa, H. Zhu, K. Hashimoto, H. Kishihara, R. Kubo, T. Usuki, and M. Okuyama, *Sens. Mater.*, **12**, 375 (2000).
4. W. Zhu, O. Tan, Q. Yan, and J. Oh, *Sens. Actuat.*, B **65**, 366 (2000).
5. X. Chen, W. Zhu, and O. Tan, *Mater. Sci. Eng*. B **77**, 177 (2000).
6. I. Vendik, O. Vendik, V. Pleskachev, and M. Nikol 'ski, *IEEE Trans. Appl. Supercond.*, **13**(2): Part 1, 716 (2003).
7. S.W. Kirchoefer, E.J. Cukauskas, N.S. Barker, H. S. Newman, and W. Chang, *Appl. Phys. Lett*., **80**(7), 1255 (2002).
8. J. Maria, C. Parker, A. Kingon, and G. Stauf, In: *Proceedings of the 13th IEEE International Symposium on Applications of Ferroelectrics, 2002*. (ISAF 2002), p. 151.
9. Z.Y. Wang, J.S. Liu, T.L. Ren, and L.T. Liu, *Sens. Actuat. A-physical*, **117**(2), 293 (2005).
10. X.J. Yang, X. Yao, and L.Y. Zhang, *Ceram. Intern.*, **30** (7), Sp. Iss. SI, 1525 (2004).
11. S.T. Chang and J.M. Lee, *Appl. Phys. Lett*., **80**(4) 655 (2002).